Geomech. Geophys. Geo-energ. Geo-resour. (2024) 10:35
https://doi.org/10.1007/s40948-023-00693-2

RESEARCH

A sustainable clean energy source for mitigating CO_2 emissions: numerical simulation of Hamit granitoid, Central Anatolian Massif

Tolga Ayzit · Mrityunjay Singh · Dornadula Chandrasekharam · Alper Baba

Received: 23 August 2023 / Accepted: 12 November 2023

Abstract Türkiye relies on coal-fired power plants for approximately 18 GW of annual electricity generation, with significantly higher CO_2 emissions compared to geothermal power plants. On the other hand, geothermal energy resources, such as Enhanced Geothermal Systems (EGS) and hydrothermal systems, offer low CO_2 emissions and baseload power, making them attractive clean energy sources. Radiogenic granitoid, with high heat generation capacity, is a potential and cleaner energy source using EGS. The Anatolian plateau hosts numerous tectonic zones with plutonic rocks containing high concentrations of radioactive elements, such as the Central Anatolian Massif. This study evaluates the power generation capacity of the Hamit granitoid (HG) and presents a thermo-hydraulic-mechanical (THM) model for a closed-loop geothermal well for harnessing heat from this granitoid. A sensitivity analysis based on fluid injection rates and wellbore length emphasizes the importance of fluid resident time for effective heat extraction. Closed-loop systems pose fewer geomechanical risks than fractured systems and can be developed through site selection, system design, and monitoring. Geothermal wellbore casing material must withstand high temperatures, corrosive environments, and should have low thermal conductivity. The HG exhibits the highest heat generation capacity among Anatolian granitoid intrusions and offers potential for sustainable energy development through EGS, thereby reducing CO_2 emissions.

Article Highlights

1. Hamit granitoid's high heat capacity is ideal for sustainable EGS energy.
2. Closed-loop geothermal wells in Hamit granitoid lowers geomechanical risks.
3. Effective heat extraction hinges on fluid dynamics and wellbore design.

Keywords Enhanced geothermal system · Geothermal exploration · Radiogenic granitoid · Closed-loop · Thermo-hydraulic-mechanical modeling · Türkiye

T. Ayzit · D. Chandrasekharam · A. Baba
Department of International Water Resources, Izmir Institute of Technology, 35430 Izmir, Turkey
e-mail: tolgaayzit@iyte.edu.tr

D. Chandrasekharam
e-mail: dornadulachandra@iyte.edu.tr

A. Baba
e-mail: alperbaba@iyte.edu.tr

M. Singh (✉)
Section 4, .8, Geoenergy, GFZ Potsdam, 14473 Potsdam, Germany
e-mail: singh@gfz-potsdam.de

Published online: 30 January 2024

1 Introduction

As the population and energy needs grow, so do the environmental problems of today. Türkiye's energy demand would increase by 93% and CO_2 emissions would increase by 25% if current consumption trends continue through 2040 (International Energy Agency (IEA) 2014, 2021). Countries supporting the Paris Agreement have already planned for nearly 30 years to reach their net-zero CO_2 emissions target. The net-zero path assumes 90% decarbonization of the power sector in Türkiye by 2040 (World Bank Group 2022). The only way to achieve this target is to increase the share of renewables in the primary energy mix. In 2020, only ¼ of the energy generated in Türkiye came from renewable energy sources (International Energy Agency (IEA) 2019, 2020). Renewable energy is an important component of sustainable development, as it is a cost-effective, environmentally friendly, and decentralized alternative to conventional energy production Within the framework of renewable energy, geothermal energy is the only energy model that does not require climate adaptation and that we can use continuously.

Heat comes from a variety of sources, including gravitational energy released during formation, the decay of naturally occurring radioactive isotopes, and the original heat from the formation of the world. The temperature rises on an average of 3 °C every 100 m from the surface to the center of the planet. The earth has a virtually unlimited heat potential, as 99% of the earth is hotter than 1000 °C (Bächler 2003). Hydrothermal reservoirs are those that are naturally hot enough and permeable, while enhanced geothermal systems are those that are naturally hot enough but developed by hydraulic excitation. Hydrothermal reservoirs are geothermal resources that are characterized by their innate ability to store and transmit heat due to naturally occurring conditions within the Earth's crust. These reservoirs are composed of porous and permeable rock formations that contain hot water or steam, which can be readily accessed through drilling. The permeability of the rock is a crucial characteristic, as it allows for the movement of geothermal fluids that can be brought to the surface to generate electricity or for direct use in heating. The term "hydrothermal" refers to the presence of water that can carry thermal energy from depth to the surface. These reservoirs typically occur in regions with volcanic or tectonic activity, where geological processes have created fractures and pathways that facilitate the flow of geothermal fluids. That is, the first approach to construct fracture networks to create conductive fluid pathways in rocks with low permeability in deep geothermal reservoirs is enhanced geothermal systems (EGS), in which a high-pressure fluid is injected (Ellsworth 2013; Olasolo et al. 2016). Considering the sustainability of improved fracture permeability, homogeneous distribution of flow between multiple parallel fractures, and induced seismicity, closed-loop geothermal systems offer numerous advantages over their open-loop counterparts. Closed-loop geothermal systems circulate heat transfer fluids through an underground network of pipes to exchange heat with the ground. They can be designed as either vertical or horizontal loops, depending on site-specific constraints and requirements. They have higher efficiency because the heat transfer fluid is enclosed in a closed loop, minimizing heat loss. The heat transfer fluid absorbs the thermal energy of the earth and high enthalpy geothermal systems can support power generation. Thermo-hydraulic-mechanical (THM) modeling is essential for closed-loop geothermal systems because it provides a more holistic approach to system design and ensures long-term reliability and efficiency.

Türkiye has many hydrothermal provinces due to the high thermal regime, with the most important high enthalpy provinces located in western and central Anatolia (Baba et al. 2014). In addition, there are many alkaline magmatic intrusions in the Anatolian plateau that have the potential to host enhanced geothermal systems (EGS) resulting from plate melting of a series of subduction zones dipping north of the Hercynian-Hellenic arc (Ayzit et al. 2022; Chandrasekharam et al. 2022a). Granitoids in regions with a similar tectonic regime and deeper Curie point depths around the world (Soultz, Cornwall) host enhanced geothermal systems (Koelbel and Genter 2017; Letcher 2020). The Alpine Mountain Belt includes plutons of different ages and compositions that are abundant in Anatolia. Plutonic rocks with high radioactive element content, directly related to alkaline magmatism, are present along the major suture zones. Türkiye has great potential to enrich its geothermal resources with radiogenic granitoids. The EGS potential should be evaluated to exploit, in particular, alkaline magmatic intrusions associated with

the Izmir-Ankara-Erzincan Suture Zone (IAESZ) as a future renewable energy source. In the present paper, it is assessed the power generation capacity of Hamit granitoid (HG), with an outcropping area of about 120 km^2 located within the west of the Central Anatolian Massif (CAM), defines the technology involved in harnessing the heat from these granitoids and a detailed thermo-hydraulic-mechanical (THM) model is developed for a closed-loop geothermal well with geological settings.

2 Geological assessment

The Anatolian plateau, located on the western Alpine-Himalayan orogenic belt, is a complex collision of the Gondwanan and Laurasian microcontinents from the Late Cretaceous to the Paleogene (Fig. 1) and is composed of several tectonic zones, which are mainly the Pontides, Anatolide Taurides, and the Central Anatolian Massif (Şengör and Yilmaz 1981; Okay and Tüysüz 1999) (Fig. 2a).

Fig. 1 Tectonic setting of Central Anatolia within the Alpine Himalayan (modified from Okay 2008; Chandrasekharam et al. 2022b)

The CAM is roughly triangular-shaped and restricted by the IAESZ to the north, the left-lateral Ecemiş fault to the east, and the right-lateral Tuz Lake fault to the west (Fig. 2b). The Central Anatolian Massif has been affected by uplifting, block-faulting, and young intracratonic over-thrusts during the closure of the Neotethyan Ocean along two north-dipping subduction zones beneath the Pontide arc at the beginning of the Late Cretaceous (Kadıoglu et al. 2006; Lefebvre et al. 2013).

2.1 Petrology of the north-western margin of CAM

The Central Anatolian Massif consists of the metamorphic crystalline massifs/complexes of Kırşehir, Akdağ and Niğde (CACC). These are Paleozoic -Mesozoic, medium- to high-grade metamorphic rocks overlain by Late Cretaceous ophiolitic units and intruded by numerous plutons ranging in age from Late Cretaceous to Miocene. The magmatic activity of the Central Anatolia region is characterized by calcareous subalkaline transitional rocks and alkaline plutonic rocks that have been influenced by crustal assimilation associated with fractional crystallization processes of similar ages in a collision-related tectonic setting since the Maastrichtian (Seymen 1983; Ilbeyli 1998).

The magmatic activity is occurred from 110 to 65 Ma, according to the age of emplacement of the plutons described in the literature (Boztuğ and Harlavan 2008; Göncüoğlu 1986; Güleç 1994; Isik et al. 2008; Köksal et al. 2012; Whitney et al. 2003). The oldest granite supersuit is forming as an outer magmatic belt in the western and northern CAM. As move towards the center, monzogranite supersuits and syenite supersuits are occurred, respectively (Kadıoglu et al. 2006).

The north-western boundary of the massif is approximately a 120-km-long strip with massive outcrops Bekrekdağ, Cefalıkdağ, Çelebi, Baranadağ and Hamit that stretches from northeast of Kırıkkale in the north to Kırşehir in the south, bending from NE-SW (Table 1).

The most common mineral phases of the Central Anatolian plutons are feldspars (plagioclase and alkali feldspar). Alkali feldspar can account for about 90% of the Hamit pluton's alkali feldspar syenite. Alkali feldspar syenite, quartz syenite, and foid monzosyenite are the most common rock types in the

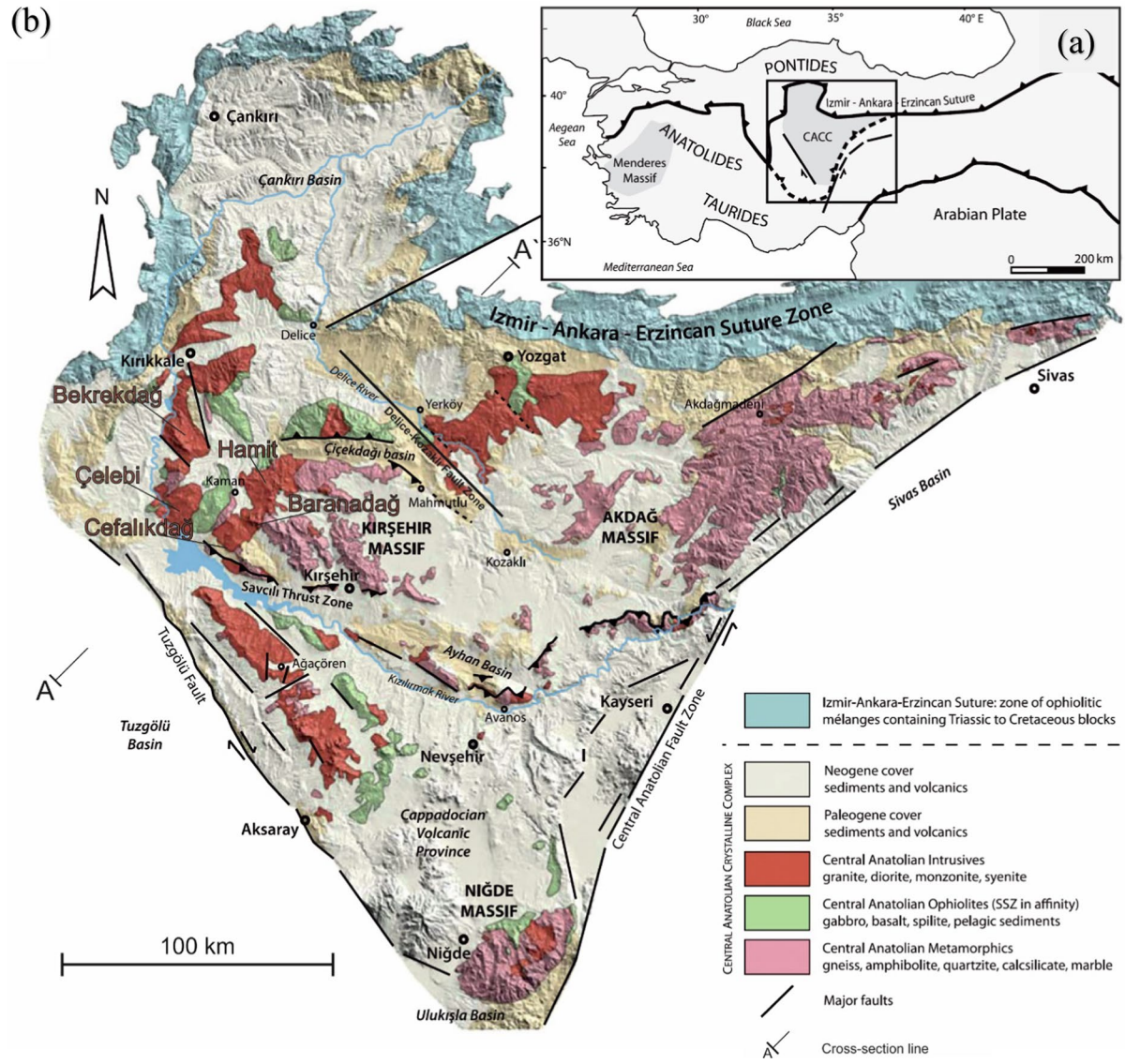

Fig. 2 **a** Tectonic zones of the Anatolian plate in general terms. **b** Simplified geological map of the Central Anatolian Crystalline Complex (CACC); (modified and combined from Lefebvre et al. 2013, 2011; Ilbeyli 1998; Advokaat et al. 2014)

Table 1 Plutonic rock types and cover areas along the north-western margin of Central Anatolian Massif; data from (Ilbeyli 1998)

Pluton name	Behrekdağ	Cefalıkdağ	Çelebi	Baranadağ	Hamit
Area (km^2)	230	76	150	65	120
Rock unit	Quartz monzonite granite	Monzodiorite, quartz monzonite, granite	Quartz monzonite, granite Monzonite, quartz monzonite		Nepheline, monzosyenite, pseudoleucite monzosyenite, alkali feldspar syenite, quartz syenite

Hamit granitoid according to Streckesisen (Streckeisen 1976) classification and the foid-bearing rocks (nepheline monzosyenite and pseudoleucite monzosyenite) are the dominating lithology. Hamit pluton has its source the lithospheric mantle that is metasomatized by subduction fluids. The foid-bearing micro-syenitic dykes cut the nepheline monzosyenite and pseudoleucite monzosyenite in E–W and NE–SW directions. The foid-bearing microsyenitic dykes are mostly phonolite including plagioclase, clinopyroxene, alkali feldspar, and nepheline phenocrysts, and present a well-developed porphyritic texture. Quartz is a late phase that fills the gaps between the other phases and is intergrown with plagioclase as well as alkali feldspar (Ilbeyli 1998).

2.2 Stress regime over the region

Extraction of heat from such highly radiogenic granitoids requires the creation of a network of fractures by the hydro fracking process. To create a horizontal fracture network, the stress regime acting on the rock mass needs to be evaluated. The structural geology of the Central Anatolia Massif is explained by the synchronized movement of the subduction zone beneath the Pontides and an intra oceanic subduction zone in the Neotethys.

The Central Anatolian Massif ~ E–W tension forces are still active since the subduction segment in the ~ N–S direction has retreated to the west since the Cretaceous (Hinsbergen et al. 2016). Central Anatolian Massif's plutons are mostly controlled by NW, WNW, and NE direction tectonic structures however the Central Anatolian magmatic belt is thought to have originated along with an NNE trending, E-dipping subduction zone (Lefebvre et al. 2013).

Hamit pluton is located between the dextral Delice-Kozaklı Fault Zone and sinistral Savcılı Thrust Zone which are NW and WNW trending, respectively (Fig. 3). As Işık et al. (2014) have stated the Savcılı Thrust Zone is delineated as a WNW-striking and SW-dipping fault carrying mostly N10 directional slicken lines. The Delice-Kozaklı Fault Zone is the right-lateral transpressional is presenting that 200 of clockwise rotation. The northwest Central Anatolian Massif is presenting a slight counter-clockwise rotation move which is 6.10 ± 3.60 (Lefebvre et al. 2013). Plutonic rocks are overlaid by circa 1 km of Cenozoic sediments at low elevations of the basin.

2.3 Curie point depth (CPD) of the Hamit granitoid

Temperature affects the properties of materials that are paramagnetic and ferromagnetic, but not those that are diamagnetic. Since there is little thermal motion at very low temperatures, the alignment of these dipoles is greatly simplified. The effective field of the material disappears abruptly at a certain temperature, and its ferromagnetic property is completely replaced by the paramagnetic one (Nagata 1961). The Curie temperature is described by the change from

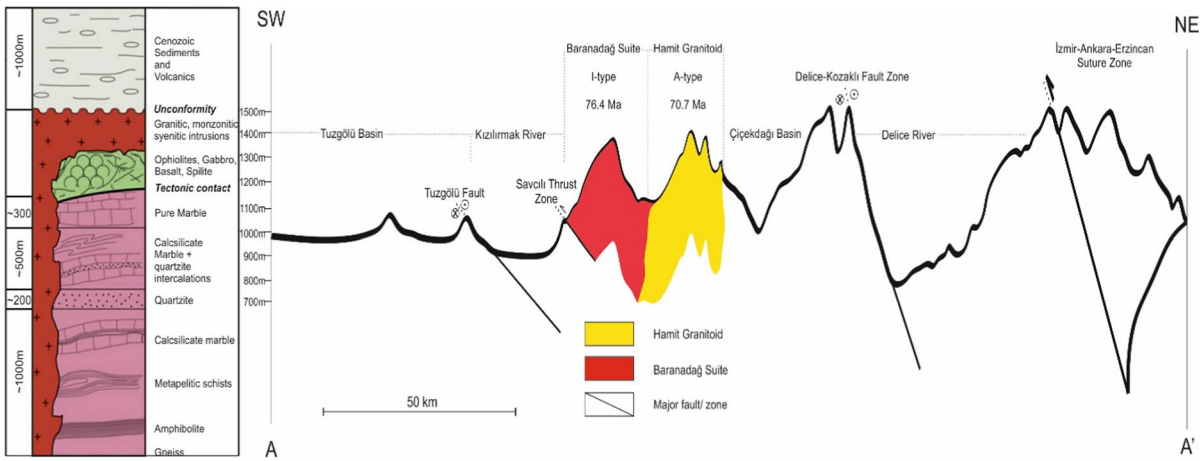

Fig. 3 Lithostratigraphic column section of CAM (not to scale); (modified from Lefebvre et al. 2011) and the north-east direction cross-section between Tuzgölü Basin and IAESZ which is a boundary between Pontides and CAM

ferromagnetic to paramagnetic equilibrium, which was discovered by Pierre Curie. The Curie temperature does not correspond to the temperature at which magnetic susceptibility disappears, but rather to a second-order phase transition with an inflection point at which susceptibility is potentially unbounded (Petrovský and Geodaetica 2005). Therefore, the depth associated with this temperature is a measure of the magnitude of the magnetic sources.

The Curie temperatures of different ferromagnetic minerals vary, and the magnetic titanomagnetite ($Fe_{2\cdot4}Ti_{06}O_4$) mineral, which is particularly prevalent in the crust, is used as the foundation for calculating the Curie point depth. Generally, aeromagnetic data is used to calculate Curie point depth and at a temperature of 580 °C reaches the curie point, where it begins to acquire paramagnetic properties (Haggerty 1978; Schlinger 1985; Frost and Shive 1986).

Depending on the local geology and rock composition, the Curie-point temperature changes from one area to another. Therefore, it is typical to expect shallow Curie-point depths in areas with geothermal potential and thin crust. The Central Anatolia lithosphere's thermal structure, particularly its viscoelastic strength, can be characterized using knowledge of the Curie isotherm's depth (Quintero et al. 2019).

As a result of the Curie point depth studies carried out in Central Anatolia, it was calculated as an average of 15.4 km between 7.9 and 22.6 km. The Hamit granitoid was calculated in the range of approximately 12–14 km using aeromagnetic anomalies in the region (Ates et al. 2005). The minimum Curie point depth is observed in the basin west of the Hamit granitoid and the shallow Curie point depth direction is approximately northeast (Fig. 4). The northern portion of Central Anatolia appears to have a Curie point depth that is 2 km shallower than the southern portion (Ayzit et al. 2022; Chandrasekharam et al. 2022a, 2022b; Uğur and Yahya 2011).

3 Radiogenic characteristics and EGS potential of the Hamit granitoid

Granitoids are the primary hosts of the key radiogenic elements U, Th, and K in the crust. Granitoids have a direct impact on the upper crust's surface heat flow and geothermal regime (Jaupart et al. 2016; Mareschal and Jaupart 2013; McLaren et al. 2006). The quantity and distribution of radiogenic components in granitoids are used to estimate heat generation capacity and geothermal source potential (Ayzit et al. 2022; Pleitavino et al. 2021). Rybach's Eq. (Pleitavino et al. 2021) was used to calculate the heat generation rate (A).

Each equation should be shown on its own line and carry a number (in consecutive order) on the right margin, in squared brackets, as shown below.

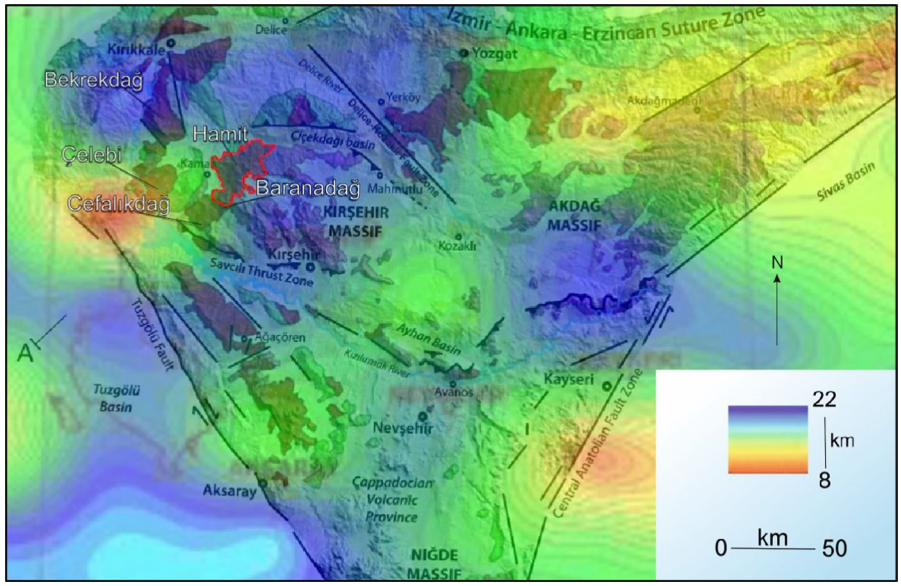

Fig. 4 Curie point depth map of Central Anatolian Massif (modified and combined from Lefebvre et al. 2013, 2011; Ilbeyli 1998; Chandrasekharam et al. 2022b; Advokaat et al. 2014; Aydin et al. 2005)

$$A\left(\mu W/m^3\right) = 10 - 2 * \rho * \left(9.52C_U + 2.56C_{Th} + 3.48C_K\right) \quad (1)$$

where ρ (g/cm^3) is the density of the rock (average density for granitoid is 2.7 g/cm^3), and C_U, C_{Th} and C_K are the concentrations of uranium (ppm), thorium (ppm), and potassium (%), respectively. C_K is expressed as a percentage of elemental potassium (or K_2O multiplied by 0.83). The surface heat flow values were calculated using the equation (Lachenbruch 1968).

$$Q = Q_0 + D * A \quad (2)$$

where Q is the heat flow at the surface, Q_0 is an initial value of heat flow unrelated to the specific decay of radioactive element at a certain time, D is the thickness of rock over which the distribution of radioactive element is just about homogeneous, and A is the radioactive heat production. Since the thin crustal thickness (~30 km) is observed in the north-western margin of the Central Anatolian Massif (Tezel et al. 2013), the background heat flow value of 40 mW/m^2 is considered around Hamit granitoid.

The Kırşehir Massif region in the west of Central Anatolia has several plutons that are extremely radiogenic due to the contents of high concentrations of uranium, thorium, and potassium minerals (Table 2).

The heat generation capacity of the Hamit granitoid can reach up to 21.48 (μW/m^3), which is much higher than the average production value of the continental crust (5 μW/m^3). Also, the heat flow value for this granitoid is approximately 254.8 mW/m^2 (D = 10 km), which is the highest heat flow value calculated in Türkiye so far.

Due to their high heat-generating capability and enabling the production potential of base-load power for societal usage, radiogenic high heat-generating granitoids are being considered as a future energy source. Considering the heat flow values, heat generation values, the probable volume of the

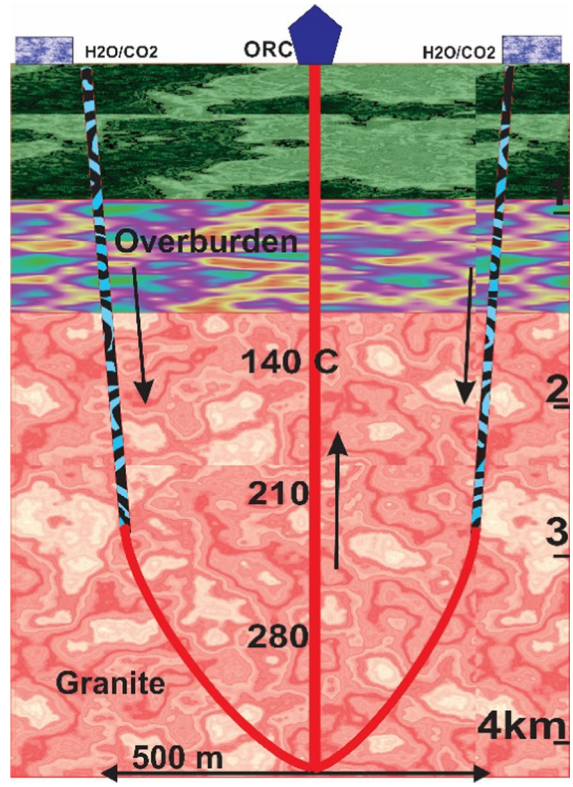

Fig. 5 Closed-loop system concept that can be applied for the Hamit granitoid region

Table 2 Late Cretaceous plutonic rock's geochemical descriptions and radioactive heat production (μW/m^3) value along the north-western margin of Central Anatolian Massif

Pluton name	Average curie point depth (km)	Rock type/geochemical description	Th (ppm)	U (ppm)	K (%)	Radioactive heat production (μW/m^3)	Heat flow (mW/m^2)
Behrekdağ	17–19	gr/qmz	37.2	5.4	3.8	4.3	83.2
Cefalıkdağ	9–11	qmz/qmz	23.1	5.1	3.9	3.3	72.7
Çelebi	8–10	gr/gr	43.5	8	4.3	5.5	94.6
Baranadağ	11–13	qmz/qmz	55.4	14.1	4.6	7.9	118.8
Hamit	12–14	pho/fsy	135.5	44.7	6.6	21.5	254.8

qmz quartz monzonite, *gr* granite, *pho* phonolite, *fsy* foid syenite (combined data from Ilbeyli 1998; Uğur et al. 2014; Aydin et al. 2005)

granitoids, and the curie depth temperature of this region, the Hamit pluton is a great site for initiating the EGS project. Firstly, the closed-loop geothermal system concept that can be applied to the Hamit granitoid region should be discussed with its mechanisms (Fig. 5).

4 The reservoir numerical simulation of closed-loop geothermal system

Several modeling techniques have been developed and applied to the analysis and design of closed-loop geothermal systems (Schulz 2008; Fallah et al. 2021; Wang et al. 2021a, b; Dornadula et al. 2023). These techniques include analytical models, numerical models, and hybrid approaches. Analytical models provide an expedited understanding of system behavior through simplified mathematical equations, while numerical models are more detailed and flexible, accounting for the complexity of heat transfer and fluid flow processes in the subsurface. Hybrid approaches combine the strengths of analytical and numerical models to optimize system performance and minimize computational effort.

Hydrothermal modeling plays a crucial role in the design and optimization of closed loop geothermal systems (Budiono et al. 2022). This approach focuses on simulating the heat transfer processes between the heat transfer fluid and the surrounding ground, considering factors such as thermal conductivity, heat capacity, and fluid flow rates. Recent advances in hydrothermal modeling have led to provide incorporating the effects of groundwater flow, accounting for complex geological structures, and implementing advanced numerical methods to solve governing equations. These advancements have allowed for more accurate system designs, leading to increased efficiency and reliability of closed loop geothermal systems.

Thermo-hydro-mechanical (THM) modeling is essential for closed loop geothermal systems because it provides a comprehensive understanding of the complex interactions occurring in the subsurface environment (Dornadula et al. 2023; Rinaldi et al. 2015; Rutqvist 2012; Rutqvist et al. 2008, 2002). In these systems, heat transfer, fluid flow, and mechanical stresses are interdependent, resulting in coupled processes that can influence the overall performance and stability of the geothermal installation.

4.1 Modeling methodology

The method consists of a numerical model for a closed-loop geothermal system in the Hamit granitoid region, focusing on the fully coupled thermo-hydro-mechanical (THM) processes and employing the finite element technique for discretization using COMSOL Multiphysics (Multiphysics 2020). The development of a numerical model provides a comprehensive understanding of the complex interplay between fluid flow, heat transfer, and mechanical deformation in the geothermal system.

The numerical model incorporates the Hamit granitoid region's geological characteristics, such as the subsurface rock formations, thermal gradients, and in-situ stress conditions, to ensure a realistic representation of the geothermal system's behavior. Additionally, the model accounts for the region-specific thermal and mechanical properties of the working fluid and the surrounding rock formations, which significantly influence the overall system efficiency and lifespan. This comprehensive approach enables the identification and optimization of key design parameters such as well length, and fluid injection and production rates, ultimately contributing to improved system performance and sustainability.

To understand the effect of THM processes during a closed loop geothermal well installation model at Hamit granitoid region, a three-dimensional geometry is considered which is 35 km long, 35 km wide and 5 km deep as shown in Fig. 6a. The size of the geometry is considered to include the stress redistribution impact by the geothermal wells on the nearby naturally faulted zone. Geological settings, petrophysical, petrographical and thermophysical parameters considered for this modeling are shown in Table 3. To shed light on the design of geothermal system at region, closed loop geothermal well technology is adopted. The wells are of different length and in order to enhance the heat exchange between the rock mass the flowing fluid. Figure 6b shows three components of the closed loop geothermal well. Section A in mainly used for injecting cold water and four different lengths of section B is considered to enhance the fluid resident time in the wellbore. Section C is used

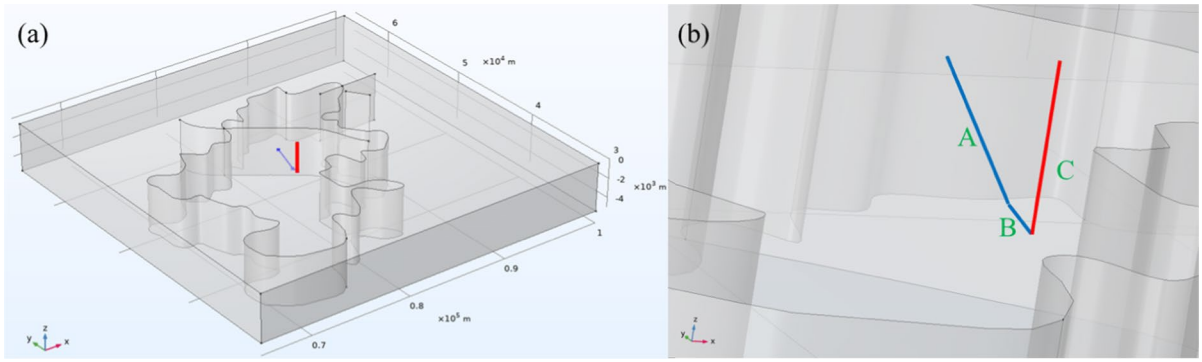

Fig. 6 **a** Three-dimensional geometry of the Hamit granitoid region used for numerical modeling. Three major fault zones are naturally present in this region. A closed loop well design is considered in this study. **b** A zoomed version of the geometry indicating the well alignment in the modeled geothermal reservoir. The blue line indicates injection well comprising two sections, A and B in which section B provides larger fluid resident time being a slightly more horizontal section compared to section A. The red line indicates production well

Table 3 Parameters employed for conducting thermo-hydro-mechanical simulations (Schulz 2008; Mahmoodpour et al. 2022; Çiftçi 2013)

Symbol	Parameter	Range
E	Young's modulus	50 GPa
ν	Poisson's ratio	0.25
ρr	Rock density	2600 $\frac{kg}{m^3}$
ϕr	Rock porosity	0.05
kr	Rock permeability	1 mD
ϕf	Fracture zone porosity	0.5
Ap	Fault zone aperture	10 m
wr	Wellbore radius	0.12 m
λr	Rock thermal conductivity	3 $\frac{W}{m\times K}$
λf	Fracture thermal conductivity	2.5 $\frac{W}{m\times K}$
Cr	Rock specific heat capacity	800 $\frac{J}{kg\times K}$
Cf	Fracture zone specific heat capacity	800 $\frac{J}{kg\times K}$
Ti	Rock compressibility	4×10^{-10} $\frac{1}{Pa}$
α	Biot coefficient	0.7
β	Thermal expansion coefficient	10^{-5} $\frac{1}{K}$
Tj	Injection temperature	30 °C
m_i	Injection mass flow rate	1, 10, 50, 100, 200, 300 kg/s
m_p	Production mass flow rate	1, 10, 50, 100, 200, 300 kg/s

for producing the hot water. The length of section A is 2500 m whereas that of section C is 3000 m. Four different lengths of section B are considered in this study: 500 m, 1 km, 2 km and 5 km.

Finite element formulation is employed to address mass conservation, energy conservation, and stress equations concurrently. Comprehensive information on governing equations is available in Mahmoodpour et al. (2022) and Singh et al. (2023). To solve these equations, COMSOL Multiphysics v5.6 (Multiphysics 2020) is utilized. Roller boundary conditions are designated to the side walls, displacement restriction is applied to the bottom boundary, and the top boundary is given free displacement. Elastic geomechanical stresses are assumed. The side boundaries allow fluid flow, while the top and bottom boundaries are

designated as no-flow for mass. A 0.254 W/m^2 constant heat flux is applied to the bottom surface, and the top surface is defined as a no-heat-flow boundary. The model's thermal gradient is 60 °C/km, with a surface temperature of 20 °C. An initial temperature field is developed based on the geothermal gradient and site's earth surface temperature. Hydrostatic pressure distribution is used to approximate the initial pore pressure. It is assumed that the geothermal system is saturated with water before injection or production commences. Initial stress values for the region are sourced from Çiftçi (2013).

Water's thermophysical properties, the working fluid for this geothermal site, are described in Singh et al. (2023). The numerical model is validated in Mahmoodpour et al. (2022), and a satisfactory match with operational data is obtained (Mahmoodpour et al. 2021). Unstructured meshing is adopted to discretize the geothermal reservoir. To counteract numerical diffusion due to mesh resolution, the wellbore's maximum mesh size is set to 1 m, significantly smaller than the fault zone aperture (10 m). Free tetrahedral meshes are used to discretize the entire domain, free triangular meshes for the fault zone, and edge elements for the wellbore geometry. The number of mesh elements varies depending on the type of geothermal system. All models are solved for a 30-year operational period.

4.2 Modeling results

Based on a global sensitivity analysis authors identified three key parameters influencing the energy extraction from a discretely fractured geothermal system: fracture aperture, rock matrix permeability and the wellbore radius (Mahmoodpour et al. 2022). However, for a closed-loop geothermal system, fracture aperture and rock matrix are not critically impacting the heat exchange. Therefore, wellbore radius or the injection flow rate is the main controlling parameter. Furthermore, wellbore length may also impact the heat extraction rate as longer wells will allow longer fluid resident time for the cold fluid. Therefore, a sensitivity analysis is performed based on the fluid injection rates and the wellbore length in this study. Temperature isosurface evolution in the vicinity of the closed loop is shown in Fig. 7a–c at three different times. Heat exchange is allowed only in sections A and B to extract heat from the rock whereas section C is fully insulated. A corresponding mean of combined thermoelastic and poroelastic stresses is shown in Fig. 8a–c.

The mean total stress in the vicinity of the wellbore is shown in Fig. 8a–c indicating that a small region is influenced by the heat transfer. A sensitivity study is performed for injection rate and wellbore length for the studied model and results are shown in Fig. 9. It is evident that the longer the well trajectory, the higher resident time will be available for water which ultimately results in higher production temperature. Another point to notice is that for the 500 m section B well trajectory, an increase in mass flux decreases the final production temperature at the end of 30 years. However, for longer well trajectories, higher production temperature is observed. This behavior could be attributed to the same reason that higher fluid resident time provides higher heat extraction capacity for the water.

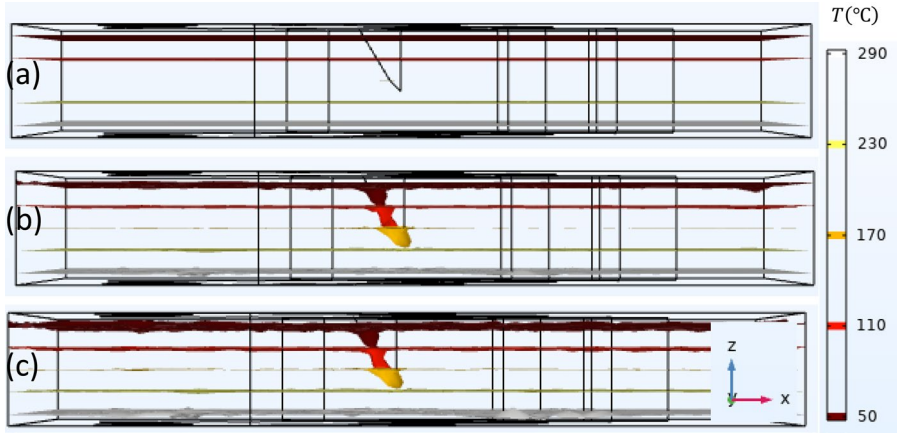

Fig. 7 Temperature development in the geothermal reservoir after **a** 1 year, **b** 5 years and **c** 30 years. Since the production well is fully insulated, there is no heat losses along the production well

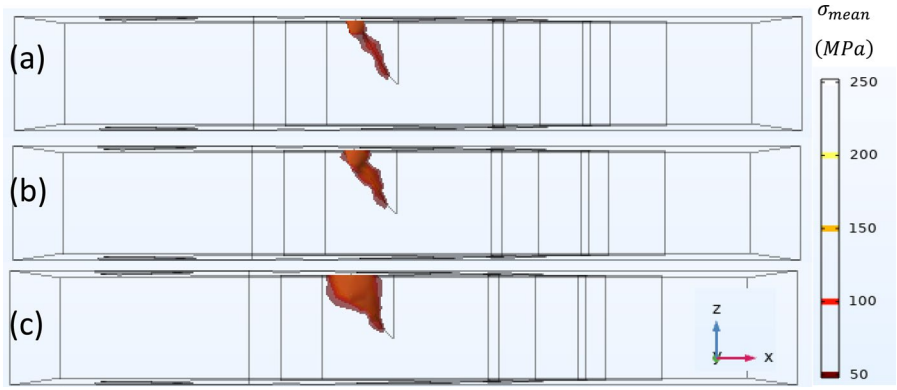

Fig. 8 Total mean stress (mean of thermoelastic and poroelastic stress) development in the geothermal reservoir after **a** 1 year, **b** 5 years and **c** 30 years

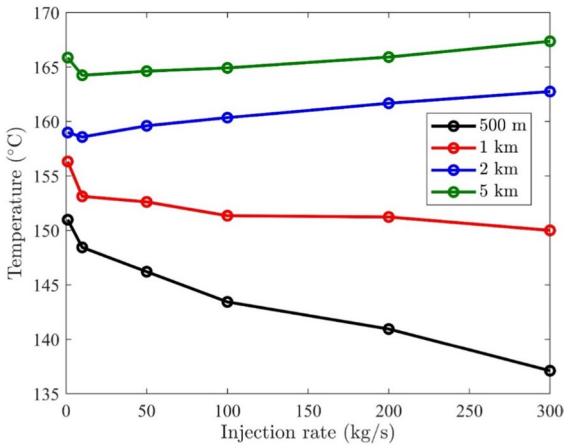

Fig. 9 Temperature at the production well after 30 years for all injection rates and four different well trajectory lengths. The legends in the figure indicate length of section B

Considering a closed-loop geothermal system at Hamit granitoid region will limit the geomechanical impacts such as fracture propagation and unwanted seismic activities for the entire operational time. Permeability changes in fractured geothermal systems can be both beneficial and detrimental to the overall performance of the system. Increased permeability can enhance convective heat transfer and improve system efficiency, while decreased permeability can reduce heat extraction rates and limit the system's capacity. Thermal, hydraulic, and mechanical factors can all contribute to changes in permeability, necessitating a comprehensive understanding of the reservoir's properties and behavior. However, in case of a closed-loop geothermal model as shown in Fig. 6 does not show any noticeable permeability change in the system.

5 Environmental effects of closed-loop geothermal systems and factors affecting its efficiency

Closed-loop geothermal systems offer several advantages over traditional open-loop systems, including reduced environmental impact, increased operational stability, and the ability to function independently of naturally occurring geothermal reservoirs. This design reduces the risk of contamination, as no groundwater is directly utilized or discharged. Moreover, closed-loop systems are often more suitable for regions with limited water resources, as they require minimal water input and have a lower environmental impact. Despite their benefits, closed-loop geothermal systems also exhibit certain limitations. The upfront costs for installation can be higher than traditional HVAC (Heating, ventilation, and air conditioning) systems, as drilling and excavation are required for loop installation. Additionally, the performance of closed loop systems can be influenced by ground conditions and soil properties, requiring careful site selection and design. Lastly, closed loop systems may require periodic maintenance to ensure optimal performance and efficiency over their operational lifespan (Schulz 2008).

Fractured geothermal systems involve the extraction of heat from underground reservoirs with high permeability and natural fractures, allowing for more efficient heat transfer through convection. In these systems, water or other working fluids flow through

the fractures, where they come into direct contact with hot rock formations. The fluid absorbs the heat and transports it to the surface, where it can be used for power generation or other applications (Schulz 2008; Rutqvist 2012; Rutqvist et al. 2008, 2002; Mahmoodpour et al. 2022; Singh et al. 2023). The convective heat transfer process in fractured systems is significantly faster than conductive heat transfers in closed-loop systems, leading to enhanced heat generation capacity.

However, for a closed-loop geothermal system, water is circulated through the pipes, and heat is transferred from the surrounding ground to the fluid via conduction. This process is relatively slow, as it depends on the thermal conductivity of the ground and the temperature gradient between the ground and the hat transfer fluid (HTF). As a result, the overall heat generation capacity of closed-loop systems is limited by the rate of conductive heat transfer.

The geomechanical impacts of closed-loop geothermal systems are generally less severe than those of fractured systems. The primary concern in closed-loop systems is the potential for ground deformation and subsidence due to the removal of heat from the subsurface. This can result in changes in stress distribution and soil compaction, which may affect the structural integrity of buildings and infrastructure near the geothermal installation. However, these geomechanical impacts are typically limited in scope and can be mitigated through careful site selection, system design, and monitoring. It should be noted that close to the wellbore trajectory, the total stress reaches a higher value due to higher injection rates. To minimize this stress, a smaller injection rate may be suitable given that the total economic output is justified. In contrast, fractured geothermal systems are subject to a range of geomechanical impacts due to their reliance on fluid flow through fractures and the associated changes in stress and temperature as investigated by Dornadula et al. (2023). These impacts can include induced seismicity, fracture propagation, and permeability changes, which can affect the performance and sustainability of the geothermal reservoir. Fracture propagation is another geomechanical impact associated with fractured geothermal systems. As fluid flows through the fractures, it can cause them to propagate and extend, potentially resulting in changes to the reservoir's permeability, heat transfer efficiency, and overall performance. Induced seismicity is a potential concern in fractured geothermal systems, as fluid injection and extraction can alter the stress state of the subsurface, potentially leading to the reactivation of existing faults or the creation of new ones.

The choice of casing material for a geothermal wellbore is critical for several reasons. Firstly, the casing material must be able to withstand the high temperatures and corrosive environments encountered in geothermal reservoirs. This is essential to ensure the structural integrity of the wellbore and to prevent the risk of casing failure, which could lead to catastrophic consequences, such as loss of well control or contamination of the surrounding environment. In addition to withstanding the harsh conditions, the casing material should also exhibit low thermal conductivity to minimize heat loss from the geothermal fluids as they are brought to the surface. This is particularly important in high-temperature geothermal systems, where maximizing energy extraction efficiency is a priority. Ignoring the heat transfer through the wellbore casing could result in several negative consequences. One significant issue would be a reduction in the overall efficiency of the geothermal energy extraction process. If the casing material conducts heat readily, a considerable amount of thermal energy will be lost to the surrounding rock formations, reducing the temperature of the geothermal fluids as they travel to the surface. This, in turn, lowers the efficiency of energy conversion systems, such as turbines and heat exchangers, leading to a decreased power output. Furthermore, excessive heat transfer through the casing could also cause thermal stresses, potentially compromising the structural integrity of the casing material. This could lead to premature failure of the casing and increased maintenance costs, making the geothermal energy extraction process less economically viable. These behaviors are necessary to keep in check while designing a closed-loop geothermal wellbore as demonstrated in this study.

6 EGS technology as a renewable energy source for mitigating CO_2 emissions

EGS technology is gaining importance due to the advancement in drilling technology and the availability of radiogenic granitoids in several countries. Several countries have implemented this technology

as shown in Table 4 and generating both electricity and heat. Based on the field, a theoretical and modeling investigation conducted during the exploration stages of the Cooper Basin EGS project, it was estimated that 1 km^3 of such high radiogenic granitoids can generate about 79×10^6 kWh of electricity (Chandrasekharam et al. 2015; Somerville and Wyborn 1994; Cooper et al. 2010). The Hamit granitoid, being a batholith, with a surface area of 120 km^2, extends to several kilometers below the surface. Thus 1 km thick granitoid at 3 km depth with a volume of 120 km^3 will be able to generate about 9 billion kWh of electricity. At least 2% of this energy can be extractable (Somerville and Wyborn 1994) which is equal to 189.6 million kWh which reduces CO_2 emissions by about 189.6 million kg. Since Hamit pluton is located over the region with high heat flow and with a curie point depth of ~ 12 km (Uğur et al. 2014; Aydın et al. 2005), the leveled cost of electricity generated from such granitoid will be comparable (8 euro cents/kWh) with the cost of electricity generated from fossil fuels based energy sources (7 euro cents/kWh) (Baba and Chandrasekharam 2022). These costs are based on drilling to a depth of about 5 km. But since the depth of drilling is sallow in the case of the western Anatolian region (Baba and Chandrasekharam 2022) and Hamit granitoid, in particular, the cost of electricity will be much lower than 7 euro cents/kWh. If a closed-loop heat extraction method is adopted instead of creating a network of fractures in the granitoids at 3 km depth, as is followed traditionally in the earlier EGS projects like that followed in Soultz, France, the unit cost of power can further be reduced (Chandrasekharam et al. 2022a).

Table 4 EGS projects in operation (*power plants under construction)

EGS project	Power plant type	Flow rate (L/s)	Installed (MWe)	Thermal
Landau, Germany	ORC	80	3.6	5
Soultz, France	ORC	30	1.5	N
Altheim, Germany	ORC	81	1	12
UDDGP*	ORC	60	3	30

UDDGP United Down Deep Geothermal Project, *ORC* organic Rankine cycle (adapted from Baba and Chandrasekharam 2022; Ledingham et al. 2019; Breede et al. 2013)

7 Discussion

The scenarios produced as a result of the research show that the world's population, energy demand and therefore CO_2 emissions will increase rapidly day by day. Fossil fuel-based power plants are the main source of CO_2 emissions in Türkiye, which can be reduced by developing renewable energy technologies. Hydrothermal source can save about 32,211 million kg (~ 32 million tonnes) of CO_2 by replacing an equivalent amount of fossil fuels (about 400 million tonnes) as the main energy source (Ayzit et al. 2022; Chandrasekharam et al. 2022a).

On the other hand, since 1965, Europe has followed the strategy of consuming natural gas and renewables instead of coal, even though natural gas resources are limited. Although Europe has reduced its energy supplies from Russia since 2020, Russia currently supplies 25% of its oil needs, 46% of its coal needs, and 40% of its gas needs. Especially since February 2022, the serious tensions with Russia, with which it was not possible to reach an agreement on political issues, had a negative impact on energy supplies, and this situation had a negative effect on European energy prices. This situation showed that countries need to invest more in renewable energy to become more independent and pave the way for technological research in renewable energy. Considering climate adaptation, 24/7 applicability, small land footprint (Table 5), ability to provide baseload power, and highest efficiency in power generation, it is obvious that geothermal energy technologies are the fastest and most sustainable solution.

EGS has the opportunity to provide renewable energy to the Earth because it is an adaptable, endless, and local source. The EGS operating process can provide CO_2 sequestration, uses little water, emits less CO_2, and provides reliable baseload power as well as a "brine mining" environment for extracting critical raw materials (e.g., Li, Sr, B, REE, etc.) from the waste stream. Deep-well drilling technology and material improvements could reduce the cost of EGS technology, and geothermal energy could eventually contribute significantly to a net-zero energy system (Fig. 10). EGS energy costs (Table 5), currently around 6–9 cents/kWh, could very likely be much lower given the thermal conditions in western and central Anatolia. It was announced that the highest geothermal base temperature in Türkiye was reached

Table 5 Levelised cost of power, land footprints for 1 MMe of energy facilities and CO_2 emissions by energy sources (adapted from International Energy Agency (IEA) 2021; Chandrasekharam et al. 2016, 2018, 2022a; Chandarasekharam and Aref 2014)

Energy supply	Land footprint (hectare)/1 MMe	Levelised cost euro cents/kWh	CO_2 emissions (kg CO_2/MWh)
EGS	0.4	6–9	67
Geothermal	0.4	8	67
Wind	1.6	7.3	31
Solar photovoltaic	3.2	13	71
Thermal power plant (coal)	3.6	7	953

in the 2021 wells drilled in the Central Anatolian Massif. According to the 3SKALE energy company (2023), 341 degrees Celsius was reached at a depth of 3957 m.

Unfortunately, it is inevitable that the problem of water security will be the main problem of the world in the coming years. Seawater can be desalinated and the problem of water security is solved by using renewable energy sources with low carbon emissions. However, after the enhanced geothermal systems have been improved with technology, wastewater and desalination may be integrated into the same system and a new generation of renewable energy technology can be developed more economically and cleaner for sustainable development. Enhanced geothermal systems may satisfy the need for water-energy-food-environment security as long as the earth's core continues to cool.

8 Conclusions

The west of Central Anatolia hosts many plutons that are highly radiogenic due to the high concentration of uranium, thorium, and potassium minerals. These high heat-generating granitoids spread over an area of almost 650 km^2 between Kırşehir and Kırıkkale, in the Kırşehir Massif region. Hamit granitoid has

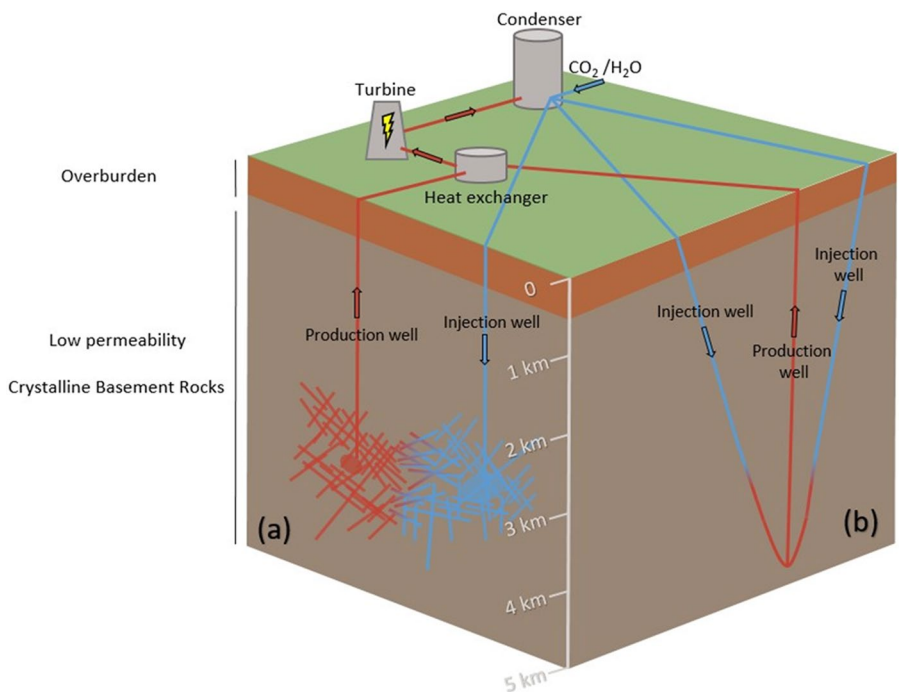

Fig. 10 **a** Schematic of a conceptual two-well enhanced geothermal system (EGS) in hot dry rock in a low-permeability crystalline basement formation and **b** Drilling in hard dry rock that lacks natural cracks and connecting between the wells via close-loop technology

the highest heat generation potential in the region. The heat generation capacity of the Hamit granitoid can reach up to 21.48 ($\mu W/m^3$), which is much higher than the average production value of the continental crust (5 $\mu W/m^3$). Also, the heat flow value for this granitoid is 254.8 mW/m^2, which is the highest heat flow value calculated in Türkiye so far. Practically it may not be possible to extract the entire heat in place in the Hamit granitoid. Based on the earlier EGS projects, it is estimated that 2% of this heat can be extracted for use. This amounts to 189.6 million kWh. This will help the country to reduce 189.6 million kg of CO_2 emissions and comply with the Paris 2015 agreement on reducing CO_2 emissions. This energy can be utilized for generating electricity for direct applications like space cooling and heating or greenhouse cultivation. To investigate one such idea, a fully coupled thermo-hydro-mechanical model of a closed loop geothermal model is developed in this study for the Hamit granitoid. In this study, the influence of key parameters on energy extraction from closed-loop geothermal systems was investigated. Results showed that wellbore radius, fluid injection rate, and wellbore length are the primary controlling factors, with longer well trajectories resulting in higher production temperatures. The geomechanical impacts of closed-loop systems are generally less severe than those of fractured systems, with ground deformation and subsidence being the primary concerns. However, these impacts can be mitigated through careful site selection, system design, and monitoring. In comparison, fractured systems are subject to induced seismicity, fracture propagation, and permeability changes, which can affect the performance and sustainability of the reservoir. Casing material selection is critical for geothermal wellbores, as it must withstand high temperatures, corrosive environments, and exhibit low thermal conductivity to minimize heat loss. Ignoring heat transfer through the wellbore casing can lead to reduced energy extraction efficiency, lower power output, and increased maintenance costs. Careful consideration of these factors is essential for the successful design and operation of closed-loop geothermal systems. This study indicates that a closed loop geothermal system will be a suitable idea to harness geothermal energy from Hamit granitoid and similar geological regions with high geothermal gradient. Thus, a future sustainable development strategy can be adopted by utilizing this green renewable energy by the country.

Acknowledgements This paper is part of the EGS project funded by TUBITAK (project No.: 120C079) through a fellowship grant to DC.

Author contributions TA: designed the study, collected data, and wrote the manuscript. MS: designed the study, numerical modeling, and wrote the manuscript. DC: designed the study, collected data, edited the manuscript, and supervision. AB: designed the study, edited the manuscript, supervision.

Funding The work was not funded.

Availability of data and materials The data is obtained from literature and therefore no new data is produced.

Declarations

Ethics approval and consent to participate Not applicable.

Consent for publication All the authors agree to publish the article.

Competing interests The authors declare that they have no competing financial interests or personal relationships that could influence the work reported in this paper.

References

Advokaat EL, van Hinsbergen DJJ, Kaymakci N, Vissers RLM, Hendriks BWH (2014) Late Cretaceous extension and Palaeogene rotation-related contraction in Central Anatolia recorded in the Ayhan-Büyükkışla basin. Int Geol Rev 56:1813–1836

Ates A, Bilim F, Buyuksarac A (2005) Curie point depth investigation of central Anatolia, Turkey. Pure Appl Geophys 162:357–371. https://doi.org/10.1007/S00024-004-2605-3/METRICS

Aydin I, Karat HI, Koçak A (2005) Curie-point depth map of Turkey. Geophys J Int 162:633–640

Ayzit T, Chandrasekharam D, Baba A (2022) Salihli Granitoid, Menderes Massif, Western Anatolia: a sustainable clean energy source for mitigating CO_2 emissions. Springer, Berlin, pp 272–283. https://doi.org/10.1007/978-3-031-04375-8_31

Baba A, Chandrasekharam D (2022) Geothermal resources for sustainable development: a case study. Int J Energy Res. https://doi.org/10.1002/ER.7778

Baba A, Bundschuh J, Chandrasekharam D (2014) Geothermal systems and energy resources: Turkey and Greece. CRC Press, Boca Raton

Bächler D (2003) Coupled thermal-hydraulic-chemical modelling at the Soultz-sous-Forêts HDR reservoir (France)

Boztuğ D, Harlavan Y (2008) K-Ar ages of granitoids unravel the stages of Neo-Tethyan convergence in the eastern Pontides and central Anatolia, Turkey. Int J Earth Sci 97:585–599

Breede K, Dzebisashvili K, Liu X, Falcone G (2013) A systematic review of enhanced (or engineered) geothermal systems: past, present and future. Geotherm Energy 1:1–27

Budiono A, Suyitno S, Rosyadi I, Faishal A, Ilyas AX (2022) A systematic review of the design and heat transfer performance of enhanced closed-loop geothermal systems. Energies 15:742

Chandarasekharam D, Aref L (2014) CO_2 mitigation strategy through geothermal energy, Saudi Arabia. Renew Sustain Energy Rev 38:154–163

Chandrasekharam D, Lashin A, Al Arafi N, Varun C, Al Bassam A, El Alfy M, Ranjith PG, Varun C, Singh HK (2015) CO2 emission and climate change mitigation using the enhanced geothermal system (EGS) based on the high radiogenic granites of the western Saudi Arabian shield. J Afr Earth Sci. https://doi.org/10.3233/JCC-150011

Chandrasekharam D, Lashin A, Al Arifi N, Al-Bassam AM (2016) Red sea geothermal provinces. CRC Press, Boca Raton

Chandrasekharam D, Lashin A, Al Arifi N, Al-Bassam AM (2018) Desalination of seawater using geothermal energy for food and water security: Arab and Sub-Saharan countries. In: Renew. energy powered desalin. handb. Elsevier, pp 177–224

Chandrasekharam D, Baba A, Ayzit T, Singh HK (2022a) Geothermal potential of granites: case study-Kaymaz and Sivrihisar (Eskisehir region) Western Anatolia. Renew Energy 196:870–882

Chandrasekharam D, Baba A, Ayzit T (2022b) High radiogenic granites of western Anatolia for EGS: a review. EGS Futur Energy Road Ahead

Çiftçi NB (2013) In-situ stress field and mechanics of fault reactivation in the Gediz Graben, Western Turkey. J Geodyn 65:136–147

Cooper GT, Beardsmore GR, Waining BS, Pollington N, Driscoll JP (2010) The relative costs of engineered geothermal system exploration and development in Australia. In: World geotherm. congr., pp 25–29

Dornadula C, Singh M, Baba A (2023) Sahinkalesi Massif, a Resurgent Dome and Super-Hot Egs Province: Hasandag Stratovolcanic Province, Central Anatolia. Cent Anatolia. https://doi.org/10.2139/ssrn.4388412

Ellsworth WL (2013) Injection-induced earthquakes. Science (80-) 341:1225942

Fallah A, Gu Q, Chen D, Ashok P, van Oort E, Holmes M (2021) Globally scalable geothermal energy production through managed pressure operation control of deep closed-loop well systems. Energy Convers Manag 236:114056

Frost BR, Shive PN (1986) Magnetic mineralogy of the lower continental crust. J Geophys Res Solid Earth 91:6513–6521. https://doi.org/10.1029/JB091IB06P06513

Göncüoğlu MC (1986) Geochronological data from the southern part (Niğde area) of the Central Anatolian Massif. Miner Res Tech Inst Turkey Bull 105:83–96

Güleç N (1994) Rb-Sr isotope data from the Agaçören granitoid (east of Tuz Gölü): geochronological and genetical implications, Turkish. J Earth Sci 3:39–43

Haggerty SE (1978) Mineralogical contraints on Curie isotherms in deep crustal magnetic anomalies. Geophys Res Lett 5:105–108. https://doi.org/10.1029/GL005I002P00105

Ilbeyli N (1998) Petrogenesis of collision-related plutonic rocks, central Anatolia (Turkey). Durham University

International Energy Agency (IEA) (2014) World energy outlook 2014—analysis—IEA, Paris, 2014. https://www.iea.org/reports/world-energy-outlook-2014. Accessed 11 April 2023

International Energy Agency (IEA) (2019) World energy outlook 2019. OECD, Paris. https://doi.org/10.1787/caf32f3b-en

International Energy Agency (IEA) (2020) World energy outlook 2020—analysis—IEA, Paris, 2020. https://www.iea.org/reports/world-energy-outlook-2020. Accessed 12 April 2023

International Energy Agency (IEA) (2021) World energy outlook 2021—analysis—IEA, Paris, 2021. https://www.iea.org/reports/world-energy-outlook-2021. Accessed 12 April 2023

Isik V, Lo C-H, Göncüoğlu C, Demirel S (2008) 39Ar/40Ar ages from the Yozgat Batholith: preliminary data on the timing of Late Cretaceous extension in the central Anatolian crystalline complex, Turkey. J Geol 116:510–526

Işık V, Uysal IT, Caglayan A, Seyitoglu G (2014) The evolution of intraplate fault systems in central Turkey: Structural evidence and Ar-Ar and Rb-Sr age constraints for the Savcili Fault Zone. Tectonics 33:1875–1899. https://doi.org/10.1002/2014TC003565

Jaupart C, Mareschal JC, Iarotsky L (2016) Radiogenic heat production in the continental crust. Lithos 262:398–427. https://doi.org/10.1016/J.LITHOS.2016.07.017

Kadıoglu YK, Dilek Y, Foland KA (2006) Slab break-off and syncollisional origin of the Late Cretaceous magmatism in the Central Anatolian crystalline complex, Turkey

Koelbel T, Genter A (2017) Enhanced geothermal systems: the Soultz-sous-Forêts project, pp 243–248. https://doi.org/10.1007/978-3-319-45659-1_25

Köksal S, Möller A, Göncüoglu MC, Frei D, Gerdes A (2012) Crustal homogenization revealed by U-Pb zircon ages and

Hf isotope evidence from the Late Cretaceous granitoids of the Agaçören intrusive suite (Central Anatolia/Turkey). Contrib Mineral Petrol 163:725–743

Lachenbruch AH (1968) Preliminary geothermal model of the Sierra Nevada. J Geophys Res 73:6977–6989. https://doi.org/10.1029/JB073I022P06977

Ledingham P, Cotton L, Law R (2019) The united downs deep geothermal power project. In: Proc. 44th work. geotherm. reserv. eng. Stanford Univ. Stanford, CA, USA, 2019, pp 11–13

Lefebvre C, Barnhoorn A, van Hinsbergen DJJ, Kaymakci N, Vissers RLM (2011) Late Cretaceous extensional denudation along a marble detachment fault zone in the Kırşehir massif near Kaman, central Turkey. J Struct Geol 33:1220–1236

Lefebvre C, Meijers MJM, Kaymakci N, Peynircioglu A, Langereis CG, Van Hinsbergen DJJ (2013) Reconstructing the geometry of central Anatolia during the late Cretaceous: large-scale Cenozoic rotations and deformation between the Pontides and Taurides. Earth Planet Sci Lett 366:83–98

Letcher TM (2020) Future energy: improved, sustainable and clean options for our planet. In: Futur. energy improv. sustain. clean options our planet, pp 1–792. https://doi.org/10.1016/C2018-0-01500-5

Mahmoodpour S, Singh M, Turan A, Bar K, Sass I (2021) Hydro-thermal modeling for geothermal energy extraction from Soultz-sous-Forets, France. Geosciences 11:464

Mahmoodpour S, Singh M, Mahyapour R, Tangirala SK, Bar K, Sass I (2022) Numerical simulation of thermo-hydro-mechanical processes at Soultz-sous-Forets. Energies 15:9285

Mareschal JC, Jaupart C (2013) Radiogenic heat production, thermal regime and evolution of continental crust. Tectonophysics 609:524–534. https://doi.org/10.1016/J.TECTO.2012.12.001

McLaren S, Sandiford M, Powell R, Neumann N, Woodhead J (2006) Palaeozoic intraplate crustal anatexis in the Mount Painter Province, South Australia: timing, thermal budgets and the role of crustal heat production. J Petrol 47:2281–2302

Multiphysics C (2020) v. 5.6, COMSOL AB, Stockholm, Sweden. www.comsol.com

Nagata T (1961) Rock magnetism. Maruzen Company Ltd.

Okay AI (2008) Geology of Turkey: a synopsis. Anschnitt 21:19–42

Okay AI, Tüysüz O (1999) Tethyan sutures of northern Turkey. Geol Soc Lond Spec Publ 156:475–515

Olasolo P, Juárez MC, Morales MP, Liarte IA (2016) Enhanced geothermal systems (EGS): a review. Renew Sustain Energy Rev 56:133–144

Petrovský E, Geodaetica AK (2005) Comments on "The use of field dependence of magnetic susceptibility for monitoring variations in titanomagnetite composition-a case study on basanites from the Vogelsberg 1996 drillhole, Germany." Stud Geophys Geod 49:255–258. https://doi.org/10.1007/s11200-005-0008-2

Pleitavino M, Carro Perez ME, Garcia Araoz E, Cioccale MA (2021) Radiogenic heat production in granitoids from the Sierras de Cordoba, Argentina. Geotherm Energy 9:16

Quintero W, Campos-Enríquez O, Hernández O (2019) Curie point depth, thermal gradient, and heat flow in the Colombian Caribbean (northwestern South America). Geotherm Energy 7:1–20. https://doi.org/10.1186/S40517-019-0132-9/FIGURES/10

Rinaldi AP, Rutqvist J, Sonnenthal EL, Cladouhos TT (2015) Coupled THM modeling of hydroshearing stimulation in tight fractured volcanic rock. Transp Porous Media 108:131–150

Rutqvist J (2012) Fractured rock stress-permeability relationships from in situ data and effects of temperature and chemical-mechanical couplings. Crustal Permeability, pp 65–82

Rutqvist J, Wu Y-S, Tsang C-F, Bodvarsson G (2002) A modeling approach for analysis of coupled multiphase fluid flow, heat transfer, and deformation in fractured porous rock. Int J Rock Mech Min Sci 39:429–442

Rutqvist J, Freifeld B, Min K-B, Elsworth D, Tsang Y (2008) Analysis of thermally induced changes in fractured rock permeability during 8 years of heating and cooling at the Yucca Mountain Drift Scale Test. Int J Rock Mech Min Sci 45:1373–1389

Schlinger CM (1985) Magnetization of lower crust and interpretation of regional magnetic anomalies: example from Lofoten and Vesterålen, Norway. J Geophys Res Solid Earth 90:11484–11504. https://doi.org/10.1029/JB090IB13P11484

Schulz S-U (2008) Investigations on the improvement of the energy output of a Closed Loop Geothermal System (CLGS). Technical University of Berlin

Şengör AMC, Yilmaz Y (1981) Tethyan evolution of Turkey: a plate tectonic approach. Tectonophysics 75:181–241

Seymen İ (1983) Tamadağ (Kaman-Kırşehir) çevresinde Kaman grubunun ve onunla sınırdaş oluşukların karşılaştırılmalı tektonik özellikleri. Türkiye Jeol Kurumu Bülteni 26:89–98

Singh M, Mahmoodpour S, Ershadnia R, Soltanian MR, Sass I (2023) Comparative study on heat extraction from Soultz-sous-Forets geothermal field using supercritical carbon dioxide and water as the working fluid. Energy 266:126388

Somerville M, Wyborn D (1994) Energy research and development corporation (Australia), Hot dry rocks feasibility study, p 133

Streckeisen A (1976) To each plutonic rock its proper name. Earth-Sci Rev 12:1–33. https://doi.org/10.1016/0012-8252(76)90052-0

Tezel T, Shibutani T, Kaypak B (2013) Crustal thickness of Turkey determined by receiver function. J Asian Earth Sci 75:36–45

Uğur A, Yahya Ç (2011) Heat flow of the Kirşehir Massif and geological sources of the radiogenic heat production. Bull Miner Res Explor 143:53–73

Uğur A, Ulugergerli EU, Kutlu S (2014) The assessment of geothermal potential of Turkey by means of heat flow estimation. Bull Miner Res Explor 149:201–210

Van Hinsbergen DJJ, Maffione M, Plunder A, Kaymakcı N, Ganerd M, Hendriks BWH, Corfu F, Gürer D, de Gelder GINO, Peters K (2016) Tectonic evolution and paleogeography of the Kırşehir Block and the Central Anatolian Ophiolites, Turkey. Tectonics 35:983–1014

Wang G, Song X, Shi Y, Yang R, Yulong F, Zheng R, Li J (2021a) Heat extraction analysis of a novel multilateral-well coaxial closed-loop geothermal system. Renew Energy 163:974–986

Wang G, Song X, Song G, Shi Y, Yu C, Xu F, Ji J, Song Z (2021b) Analyzes of thermal characteristics of a hydrothermal coaxial closed-loop geothermal system in a horizontal well. Int J Heat Mass Transf 180:121755

Whitney DL, Teyssier C, Fayon AK, Hamilton MA, Heizler M (2003) Tectonic controls on metamorphism, partial melting, and intrusion: timing and duration of regional metamorphism and magmatism in the Niğde Massif, Turkey. Tectonophysics 376:37–60. https://doi.org/10.1016/J.TECTO.2003.08.009

World Bank Group (2022) Türkiye—country climate and development report: executive summary, Washington, DC